INCLUSION OF URBAN LANDSCAPE IN A CLIMATE MODEL

How Can Satellite Data Help?

BY MENGLIN JIN AND J. MARSHALL SHEPHERD

Urban regions, which cover only approximately 0.2% of the earth's land surface, contain about half of the human population (UNPD 2001). Modeling urban weather and climate is critical for human welfare, but has been hampered for at least two reasons: i) no urban landscape has been included in global and regional climate models (GCMs and RCMs, respectively), and ii) detailed information on urban characteristics is hard to obtain. With the advance of satellite observations, adding urban schemes into climate models in order to scale projections of global/regional climate to urban areas becomes essential. Inclusion of urbanized landscape into climate models was discussed in depth at the fall American Geophysical Union (AGU) meeting of 2003 in the session entitled "Human-induced climate variations linked to urbanization: From observations to modeling," which took place on 12 December 2003 in San Francisco, California (most of the presentations of this session can be found online at www.atmos.umd.edu/~mjin/AGU03urban.html). The following notes summarize what is known and what needs to be advanced on this topic.

AGU MEETING SESSION—HUMAN-INDUCED CLIMATE VARIATIONS LINKED TO URBANIZATION: FROM OBSERVATIONS TO MODELING

What: The unique radiative characteristics of urban land cover are now being observed by satellites, with consequent improvements possible in surface schemes of climate models
When: 12 December 2003
Where: San Francisco, California

In a GCM and RCM, land physical processes are simulated in a land surface model, which is coupled with the atmosphere model through exchanges of heat fluxes, water, and momentum. Currently, an urban classification is not included in any major GCM/RCM land surface model [e.g., the second National Center for Atmospheric Research (NCAR) Community Land Model (CLM2), National Aeronautics and Space Administration (NASA) Global Modeling and Assimilation Office (GMAO) unified land surface model, Biosphere–Atmosphere Transfer Scheme (BATS), simple Biosphere model, version 2 (SIB2), etc.]. This exclusion makes GCMs/RCMs inadequate for realistically simulating urban modifications to climate.

The same land surface model can be coupled to a GCM or RCM. For example, the NCAR CLM is coupled to both the NCAR community atmosphere

AFFILIATIONS: JIN—Department of Meteorology, University of Maryland, College Park, College Park, Maryland; SHEPHERD—NASA Goddard Space Flight Center, Greenbelt, Maryland
CORRESPONDING AUTHOR: Dr. Menglin Jin, Department of Meteorology, University of Maryland, College Park, College Park, MD 20742
E-mail: mjin@atmos.umd.edu
DOI:10.1175/BAMS-86-5-681

In final form 30 January 2005

model (CAM) as well as a regional model. Therefore, incorporating urban landscape into a land surface model is the practical way, and probably the only way, to represent urban environments in a GCM or RCM.

NEW DATA AND AVAILABILITY. Urbanization is an old topic that dates back to the 1800s (Langsberg 1981; Oke 1976). Observations from satellites, with their richness, quality, resolution, and coverage, provide a new approach for studying urban environments. Among others, NASA's *Terra, Aqua,* Landsat, and Tropical Rainfall Measuring Mission (TRMM) are especially important satellites for global and regional urban studies. For example, observations from the Moderate Resolution Imaging Spectroradiometer (MODIS) on *Terra* and *Aqua* provide nearly daily global coverage of the earth in 36 spectral bands at spatial resolutions of 1 km or better (depending on band), 4 times per day, as well as over 40 data products. Both land surface and atmosphere conditions that are modified by urban environments can now be detected from MODIS. Among others, the most important urban-related variables that can be obtained from MODIS include

a) land surface reflectance and albedo,
b) land surface emissivity,
c) leaf area index (LAI),
d) land surface skin temperature (T_{skin}),
e) land cover,
f) snow coverage,
g) cloud properties, and
h) aerosol properties.

For urban modeling purposes, the following three advantages of MODIS data make them extremely valuable:

- First, the instantaneous observations can be used to study the interaction between the land surface and its overlying atmosphere through various variables.
- Second, its global coverage enables observations of all urban pixels over the globe, identification of the extremities and median of urban impacts, and the study of the intensity of urban impacts under different climate systems or regions.
- Third, MODIS data, like those from Landsat and the Advanced Spaceborne Thermal Emission and Reflectance Radiometer (ASTER), have promising quality.

MODIS's teams have designed specific validation methods for each product via in situ field observations and algorithm intercomparisons. For example, land surface emissivity is now available for the first time globally. Although uncertainties remain over some areas, this dataset provides both global distribution and seasonal variations (Jin and Liang 2004, manuscript submitted to *J. Climate*). This product, together with emissivity data from ASTER, illustrates urban emissivity variations.

In addition, land cover, LAI, albedo, and skin temperature are globally available (Friedl et al. 2002; Wan and Dozier 1996; Myneni et al. 2002; Schaaf et al. 2002). For example, Fig. 1a shows the global distribution of land cover classification as derived from MODIS data, with Fig. 1b showing the corresponding distribution of land cover classification in the southeastern United States in the vicinity of Atlanta, Georgia. Furthermore, aerosol optical thickness, cloud optical thickness, and cloud effective radius can be used to study how urban aerosols change urban cloud microphysics (cf. Figs. 2a–c).

Daily and monthly MODIS atmosphere data are available online at http://modis-atmosphere.gsfc.nasa.gov (King et al. 2003). In addition, this site contains the surface albedo, ecosystem classification, and Normalized Difference Vegetation Index (NDVI) data that are derived from global MODIS land data, and filled in for missing data due to persistent cloud cover and seasonal snow (Moody et al. 2005). Additional land data are described and available online at http://modis-land.gsfc.nasa.gov. [These data can also be ordered through an online File Transfer Protocol (FTP) service and CDs from http://lpdaac2.usgs.gov/modis/dataproducts.esp.]

WHAT IS URBAN? Why do we need to add a new "urban" landscape in land models? Why cannot other land surface types be used to represent urban environments? To answer these questions, we have to know what are the unique physical processes and parameters of urban regions. Satellite observations help to identify these features.

With the construction of buildings, parking lots, and houses, urban areas dramatically change the smoothness of a surface (i.e., roughness length), thermal conductivity, hydraulic conductivity, albedo, emissivity, and fraction of vegetation cover. As a result, urban landscapes modify not only the original physical processes that govern any natural land surface [i.e., surface energy budget (SEB)], but also add new, unique biogeophysical and biogeochemical processes into the land surface–atmosphere, such as the storage heat flux, canyon effect, and anthropogenic heat flux. An urban scheme

a) MODIS Land Cover Classification

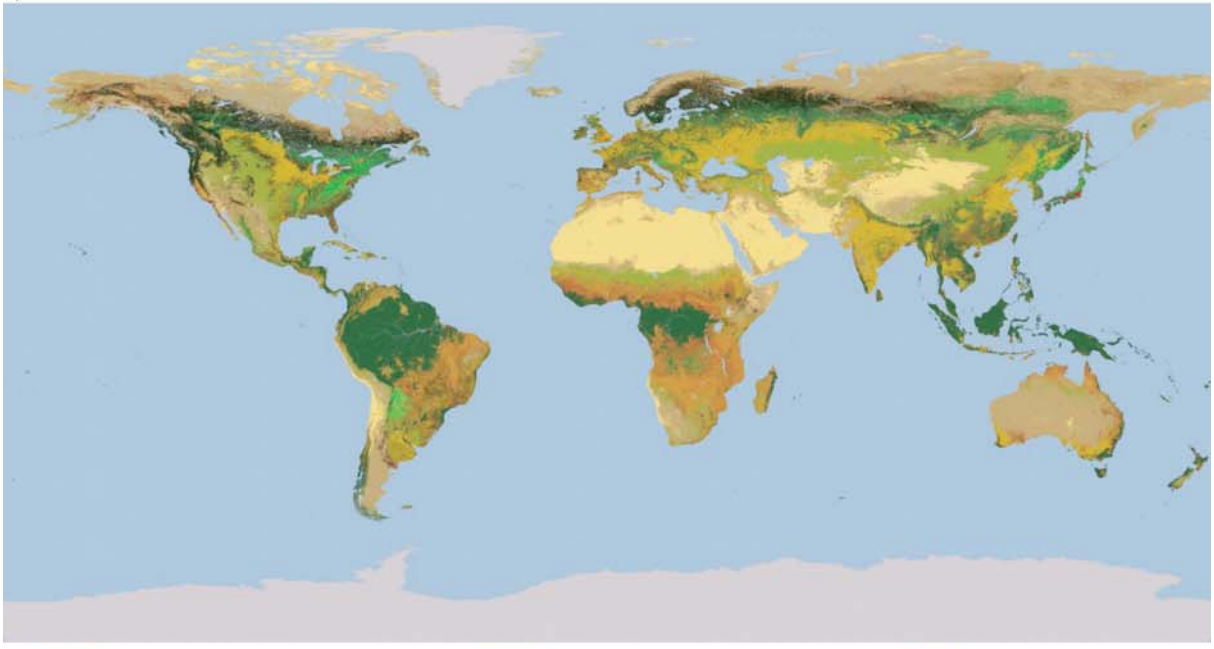

b) IGBP Classification for Southeastern US

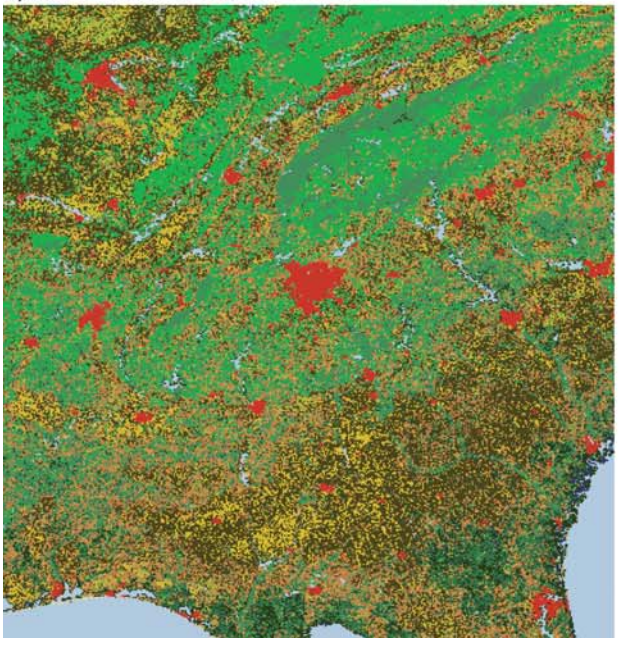

Fig. 1. (a) MODIS land cover classification. (b) MODIS land cover classification in the southeastern United States (near Atlanta, GA). Urban and built-up areas are red [land cover classification 13 in Fig. 1b provided by King et al. (2003)].

needs to reflect both the modified as well as the new processes.

By measuring spatial variations of urban and nonurban regions, satellite data help distinguish the modified properties that affect SEB, the basis on which a land surface model is built,

$$(1 - a)S_{\downarrow} + LW_{\downarrow} - \varepsilon\sigma T_{\text{skin}}{}^{4} + \text{SH} + \text{LE} + G = 0, \quad (1)$$

where SH is sensible heat flux, LE is latent heat flux, and G is the ground heat flux. These three processes compete for surface net radiation R_n, which is the downward minus upward shortwave and longwave radiation. In Eq. (1), a is surface al-

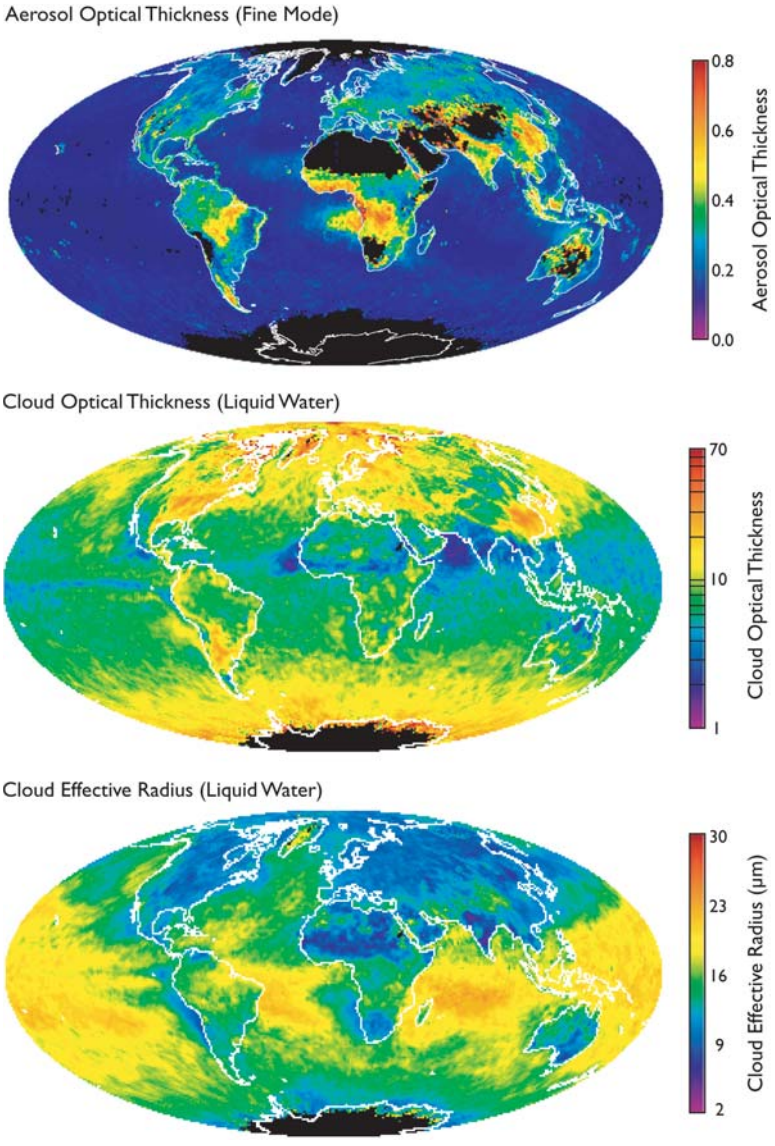

Fig. 2. (a) Global distribution of fine aerosol optical thickness derived from MODIS measurements on the *Terra* platform for Sep 2000. The large values over Southeast Asia, India, Europe, and the United States reflect urban pollution. The large values in the Southern Hemisphere are due to biomass burning. (b) Global distribution of cloud optical thickness for water clouds from *Terra* MODIS in Apr 2003. (c) Same as (b), but for effective radius. [Data obtained from M. D. King of NASA Goddard Space Flight Center (see Platnick et al. 2003).]

bedo, and $S_{\downarrow}$ is downward solar radiation; therefore, $(1 - a)S_{\downarrow}$ is reflected solar radiation. Here, $LW_{\uparrow}$ is upwelling longwave radiation from the atmosphere near the surface. Emissivity (ε) and surface skin temperature (T_{skin}) determine the upward longwave radiation, or surface emission, following the Stefan–Boltzmann law. It is evident that decreases of a and ε play important roles in surface temperature changes because input radiative energy is changed in the land surface system. In addition, the heights of buildings increase the surface "roughness length" and, thus, SH and LE are affected by enhanced surface turbulence. Furthermore, urban paved roads and concrete surfaces are waterproof, and thus, LE tends to be zero over these surfaces.

Figure 3 compares the spectral surface albedo of various land cover classifications in a region of the upper Midwest that includes Chicago, Illinois, and Indianapolis, Indiana, based on NASA Goddard Space Flight Center (GSFC) surface reflectance analysis. Urban land cover has an albedo that is lower than cropland and broadleaf forests, but higher than needleleaf forests in both the visible and near-infrared wavelengths. Because albedo accuracy affects land surface model results, accurate albedo data for urban regions are needed. Moody et al. (2005) provide more information on urban albedo.

Figure 4 shows the MODIS-measured emissivity for Beijing, China, and surrounding regions (Jin et al. 2005a). Beijing has a lower emissivity than the surrounding nonurban regions, with the minimum of 0.935 in the central part of the city. The surrounding regions have an emissivity as high as 0.96–0.97 for normal vegetative areas. The city evidently decreases the emissivity by up to 4%, which may be small in value but is large in terms of the thermal properties, because land surface emissivity varies modestly for natural surfaces—0.96–0.97 for vegetation and 0.92–0.95 for most bare soil, with extreme low values around 0.8 in deserts (Jin and Liang 2004, manuscript submitted to *J. Climate*). The 4% emissivity decrease implies a big change of land cover, suggesting that the urban environment is indeed a unique land cover classification that should be taken into account in land surface models as a separate landscape.

Urban landscape significantly affects skin temperature (cf. Fig. 5). The temperature difference of urban and nonurban areas is referred to as the

"urban heat island (UHI) effect" (Landsberg 1981). Conventionally, UHI was detected from nighttime World Meteorological Organization (WMO) 2-m surface air temperature records (T_{air}). Satellite data illustrate unique UHI features on T_{skin} as opposed to T_{air}. The T_{skin} UHI occurs during the daytime as well as at nighttime, whereas during daytime T_{skin} UHI tends to have a larger intensity than at nighttime. Such unique features are partly due to the physical differences between T_{skin} and T_{air} (Sun and Mahrt 1995; Jin et al. 1997), and partly due to the size, density, and microphysics of the city itself. More results of UHI can be found from presentations given by Milesi et al. [2003, personal communication (available online at www.atmos.umd.edu/~mjin/AGU03urban.html)], Taniguchi et al. (2003, personal communication), and Jin and Peters-Lidard (2005, manuscript submitted to *J. Hydrometeor.*).

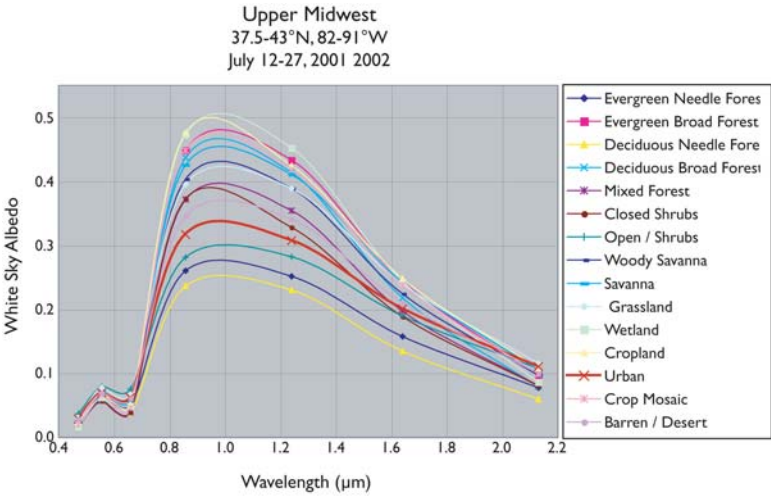

Fig. 3. The spectral distribution for various land cover types over the upper Midwest at the end of Jul 2001. The urban type is the red line, which illustrates that the urban landscape has a lower albedo than cropland and a higher albedo than forests over most wavelengths. Urban albedo has evident seasonality, with a large value in summer and a minimum value in winter (not shown). [Analysis provided by E. G. Moody and M. D. King, NASA Goddard Space Flight Center (see Moody et al. 2005).]

Satellite T_{skin} data can then be used in the two following ways for urban modeling: i) the model output can be directly compared with satellite observations to see if the model reasonably reproduces the size and intensity of UHI, and ii) satellite-derived T_{skin} can be analyzed to advance our understanding of urban thermal structure, and, thus, help improve urban parameterizations.

Urban environments change surface vegetation cover as well, which is reflected in a land surface model as LAI and fractional vegetation cover. By replacing original vegetated surface with buildings, roads, or parking lots, LAI and fractional vegetation cover are dramatically reduced. The MODIS LAI product can provide fine-resolution information between urban and nonurban regions.

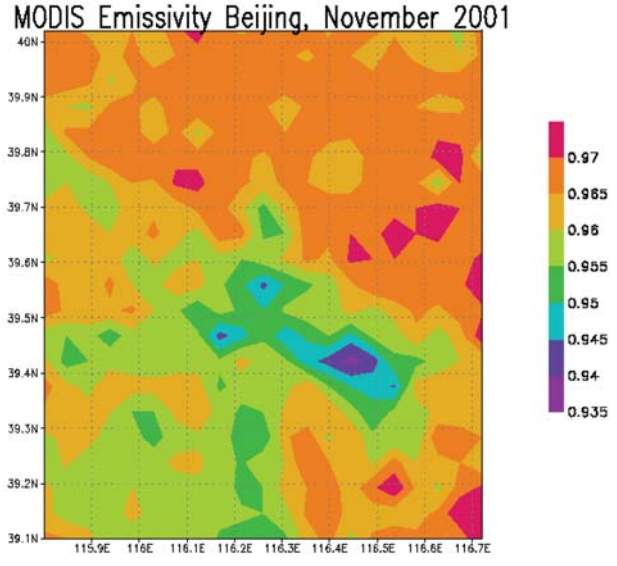

Fig. 4. Surface emissivity for Beijing, China, and surrounding regions. The low center of emissivity corresponds to the central part of Beijing. [Provided by Jin et al. 2005a.]

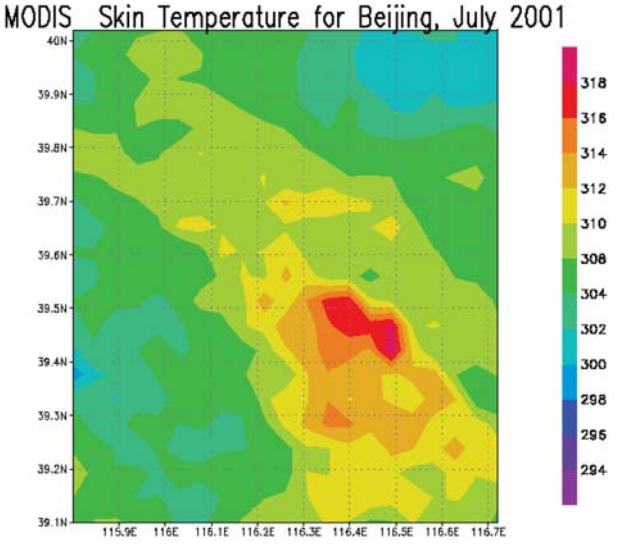

Fig. 5. Skin temperature (K) for Beijing and surrounding regions. The high-temperature center corresponds to the central part of Beijing. Data are for the daytime. [Provided by Jin et al. 2005a.]

In addition to land surface, urban areas modify atmospheric conditions. Over urban regions, the aerosol optical thickness can be as high as 0.6 (Fig. 2a), which, in turn, reduces solar insolation by about 30 W m^{-2} (direct effect). The high concentration of urban aerosol may increase downward longwave radiation partly due to its absorption and emission, and partly due to more clouds in the sky.

Aerosol–cloud interactions modify cloud properties, in particular, cloud effective radius and cloud amount, as shown in July 2001 data for the Houston, Texas, region [Fig. 6, see also Jin et al. (2005b), and A. Chu (2003, personal communication)]. The diurnal cycle of cloud properties is observed. From *Terra* observations during the morning overpass (about 1030 LST), the maximum cloud optical thickness occurred at 2.5 with an ice particle size of 25 μm, while for *Aqua* observations during the afternoon overpass (about 1330 LST), the ice particle size remained about the same; however, there were two peaks in cloud optical thickness—one at 2.5 and another at 100. Furthermore, the frequency of clouds in the afternoon was much greater than that during the morning.

Recent evidence also suggests that rainfall and the subsequent land surface hydrology are also modified by the urban environment (Rosenfeld 1999; Shepherd and Burian 2003). Figure 7 illustrates two runs from the fifth-generation Pennsylvania State University (PSU)–NCAR Mesoscale Model (MM5) NOAH land surface model in which the Houston urban surface is included (URBAN) versus not included (NOURBAN). In the NOURBAN run (right-hand panel), the urban area is replaced by cropland. In the URBAN case (left-hand panel), the apparent high surface temperatures west of Galveston Bay, Texas, represent the urban heat island. Other features of note include convection west of the UHI that seems to be enhanced and/or forced by an interaction between the sea-breeze/outflow boundaries and the boundary of the UHI. There is evidence of a convergence zone that is associated with the UHI as well. In the NOURBAN run, neither the western convective cluster nor a convergence signature in the wind (near 300 m) is evident. More on the urban impact on rainfall can be found from Andreae et al. (2004), Hooshialsadat et al. (2003, personal communication), and Wilcox (2003, personal communication).

WHAT DO WE NEED FOR MODELING URBAN REGIONS? In order to include urban effects in the land surface model, the first objective should be the development of an urban scheme that can be blended into current land surface models.

Roughness length. Probably the largest challenge in developing urban schemes is calculating the roughness length, which is a function of buildings and the combination of various urban surfaces (roads, roofs, trees, etc.). A detailed discussion of how to infer roughness length is beyond the scope of this paper, but has been discussed by Dickinson (2003, personal communication).

Urban geometry database. To calculate roughness length, we need urban building information. Global urban building density, coverage, and height information is important, but not yet available. One such prototype dataset was developed by Steve Burian (2003, personal communication) of the University of Utah for the Houston area. His urban database includes multiple surface topography and surface cover datasets, via a geographic information system (GIS). Urban canopy parameters are given in Table 1.

Updated urban cover database. The rapid increase in city size requires modelers to have an accurate global urban coverage database. The standard MODIS land cover dataset defines the urban coverage based on the Digital Chart of the World, which dates back to the 1960s. Schneider et al. (2003 a,b) have been working on developing an updated urban land cover database using MODIS pixel radiance, cloud cover, and city lights.

FINAL REMARKS. Urban schemes are currently being developed for land surface models (Dickinson 2003, personal communication). The urban schemes need to include potential feedbacks to the atmosphere and hydrological cycles. Three specific emphases that need to be considered are i) the large fraction of impervious (mostly black) surfaces that impact surface temperatures and hydrology, ii) that urban plants—either more or less than the natural background—may be irrigated, and iii) the urban transports that are generated by buildings and vegetation at multiple heights.

In conclusion, satellite-observed urban information is extremely useful for advancing our ability to simulate urban effects in climate models. Specifically, satellite data can help us to understand the diurnal, seasonal, and interannual variations of the urban surface. In addition, satellite data can specify surface parameters for a land surface model and validate the model performance.

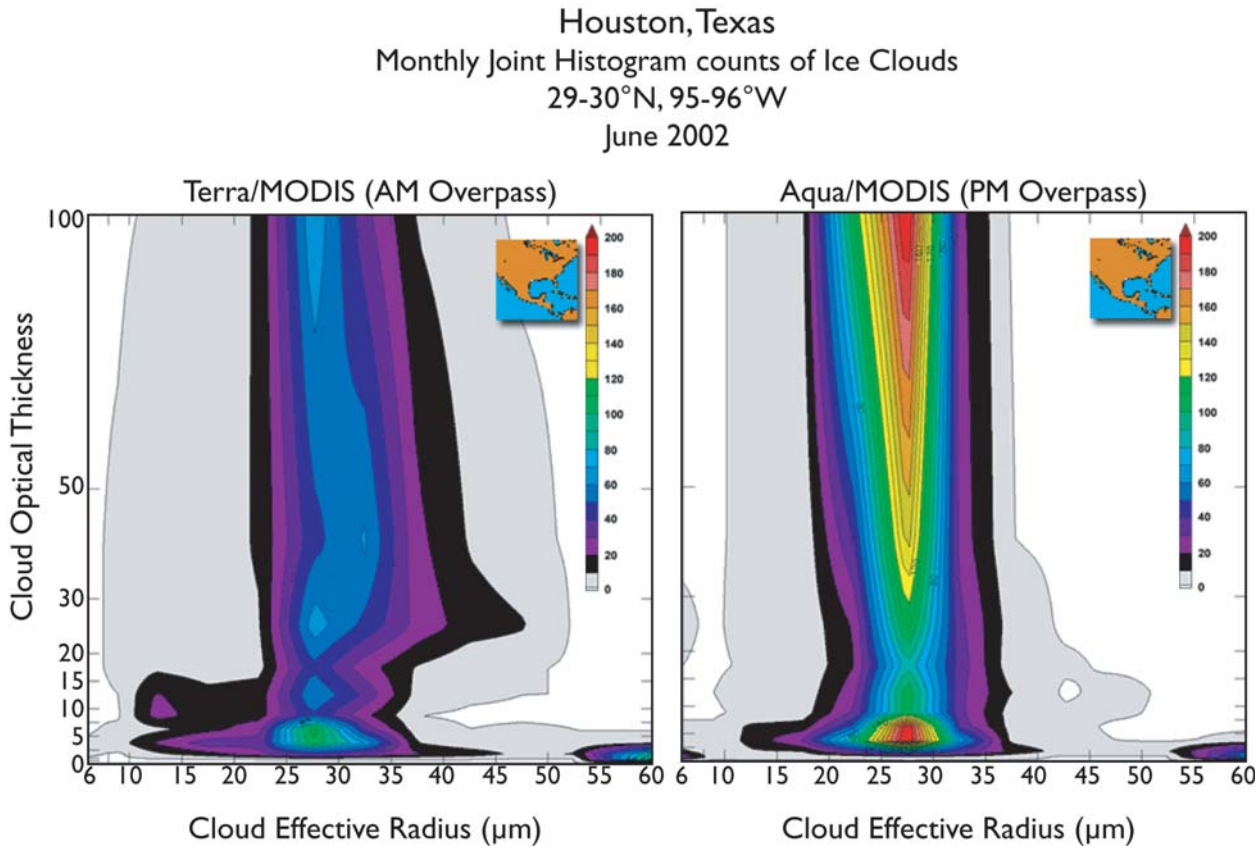

Fig. 6. Cloud optical thickness vs effective radius for water clouds from (a) *Terra* MODIS (morning overpass) and (b) *Aqua* MODIS (evening overpass). [Provided by P. A. Hubanks and M. D. King, NASA Goddard Space Flight Center.]

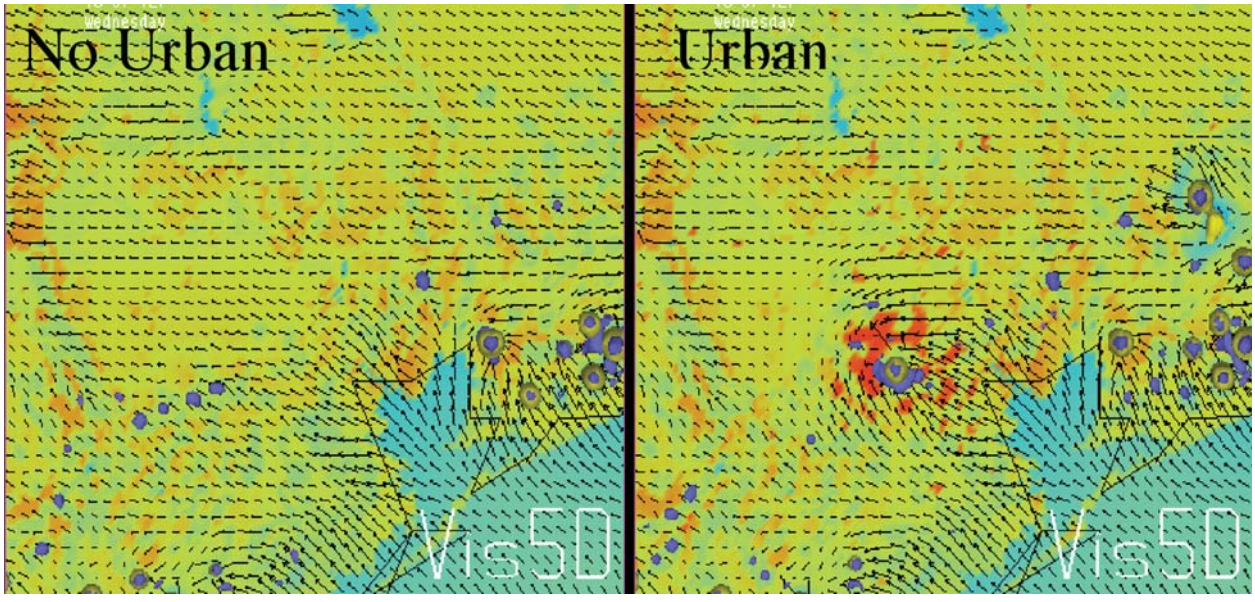

Fig. 7. MM5-NOAH simulation of 25-26 July 2001 case day for Houston, Texas: (left) nonurban case and (right) urban case. Black arrows represent wind vectors at 300m. Warm to cold colors represent surface temperature. Purple isosurfaces represent cloud water. Yellow isosurfaces represent rainwater. The time for this particular plot is 1740 UTC [Provided by Shepherd 2005.]

REFERENCES

Andreae, M. O., D. Rosenfeld, P. Artaxo, A. A. Costar, G. P. Frank, K. M. Longo, and M. A. F. Silva-Dias, 2004: Smoking rain clouds over the Amazon. *Science,* **303,** 1337–1342.

Friedl, M. A., D. K. McIver, J. C. Hodges, Y. Zhang, D. Muchoney, A. H. Strahler, C. E. Woodcock, S. Gopal, A. Schneider, A. Cooper, A. Baccini, F. Gao, and C. B. Schaaf, 2002: Global land cover mapping from MODIS: Algorithms and early results. *Remote Sens. Environ.,* **83,** 287–302.

Jin, M., R. E. Dickinson, and A. M. Vogelmann, 1997: A comparison of CCM2–BATS skin temperature and surface-air temperature with satellite and surface observations. *J. Climate,* **10,** 1505–1524.

——, ——, and D. Zhang, 2005a: The footprint of urban areas on global climate as characterized by MODIS. *J. Climate,* in press.

——, J. M. Shepherd, and M. D. King, 2005b: Urban aerosols and their interaction with clouds and rainfall: A case study for New York and Houston. *J. Geophys. Res.,* in press.

King, M., and Coauthors, 2003: Cloud and aerosol properties, precipitable water, and profiles of temperature and humidity from MODIS. *IEEE Trans. Geosci. Remote Sens.,* **41,** 442–458.

Landsberg, H. E., 1981: *The Urban Climate.* Academic Press, 275 pp.

Moody, E. G., M. D. King, S. PLatnick, C. B. Schaff, and F. Gao, 2005: Spatially complete global spectral surface albedos: Value-added datasets derived from Terra MODIS land products. *IEEE Trans. Geosci. Remote Sens.,* **43,** 144–158.

Myneni, R. B., S. Hoffman,Y. Knyazikhin, J. L. Privette, J. Glassy, Y. Tian, Y. Wang, X. Song, Y. Zhang, G. R. Smith, A. Lotsch, M. Friedl, J. T. Morisette, P. Votava, R. R. Nemani, S. W. Running, 2002: Global products of vegetation leaf area and fraction absorbed PAR from year one of MODIS data. *Remote Sens. Environ.,* **83,** 214–231.

Oke, T. R. 1976: City size and the urban heat island. *Atmos. Environ.,* **7,** 769–779.

Platnick, S., M. D. King, S. A. Ackerman, W. P. Menzel, B. A. Baum, J. C. Riti, and P. A. Frey, 2003: The MODIS cloud products: Algorithms and examples from Terra. *IEEE Trans. Geosci. Remote Sens.,* **41,** 459–473.

Rosenfeld, D., 1999: TRMM observed first direct evidence of smoke from forest fires inhibiting rainfall. *Geophys. Res. Lett.,* **26,** 3105–3108.

Schaff, C. B., F. Gao, A. H. Strahler, W. Lucht, X. W. Li, T. Tsang, N. C. Strugnell, X. Y. Zhang, Y. F. Jin, J. P. Muller, P. Lewis, M. Barnsley, P. X. Hu, S. L. Liang, J. L. Privette, and D. Roy, 2002: First operational BRDF, albedo

Table 1. The urban canopy parameters.

	Urban canopy parameter
1	Mean building height
2	Standard deviation of building height
3	Mean building height weighted by footprint plan area
4	Wall-to–plan area ratio
5	Building height-to-width ratio (λ_s)
6	Building height histograms
7	Mean vegetation height weighted by plan area
8	Mean canopy height weighted by plan area
9	Mean orientation of street
10	Building plan area density function [$A_{pb}(z)$]
11	Vegetation plan area density function [$A_{pv}(z)$]
12	Canopy plan area density function [$A_{pc}(z)$]
13	Building rooftop area density function [$A_{tb}(z)$]
14	Vegetation-top area density function [$A_{tv}(z)$]
15	Canopy-top area density function [$A_{tc}(z)$]
16	Building frontal area density function [$A_{fb}(z)$]
17	Vegetation frontal area density function [$A_{fv}(z)$]
18	Canopy frontal area density function [$A_{fc}(z)$]
19	Roughness length and displacement height
20	Roughness length and displacement height
21	Roughness length and displacement height
22	Sky-view factor
23	Plan area fraction of vegetation, buildings, water, bare soil, artificial surfaces
24	Building material
25	Directly connected impervious area (DCIA)

nadir reflectance products from MODIS, *Remote Sens. Environ.,* **83,** 135–148.

Schneider, A., M. A. Friedl, D. K. McIver, and C. E. Woodcock, 2003a: Mapping urban areas by fusing multiple sources of coarse resolution remotely sensed data. *Photogramm. Eng. Remote Sens.,* **69,** 1377–1386.

——, ——, ——, and ——, 2003b: Mapping urban areas by fusing multiple sources of coarse resolution remotely sensed data. *Photogramm. Eng. Remote Sens.,* **69,** 1377–1386.

Shepherd, M. J., 2005: A review of current investigations of urban-induced rainfall and recommendations for the future. *Earth Interactions,* in press.

Shepherd, M. J., and S. J. Burian, 2003: Detection of urban-induced rainfall anomalies in a major costal city. *Earth Interaction,* **7.** [Available online at http://EarthInteractions.org.]

Sun, J., and L. Mahrt, 1995: Determination of surface fluxes from the surface radiative temperature. *J. Amtos. Sci.,* **52,** 1096–1106.

UNPD, cited 2001: World Urbanization Prospects: The 2001 Revision. [Available online at www.un.org/esa/population/publications/wup2001.]

Wan, Z., and J. Dozier, 1996: A generalized split-window algorithm for retrieving land-surface temperature from space. *IEEE Trans. Geosci. Remote Sens.,* **34,** 892–904.